

January 1992

Stable isotope analysis using tunable diode laser spectroscopy

Todd B. Sauke

San Jose State University, todd.sauke@sjsu.edu

J. F. Becker

San Jose State University

M. Loewenstein

Ames Research Center

Follow this and additional works at: https://scholarworks.sjsu.edu/physics_astron_pub



Part of the [Astrophysics and Astronomy Commons](#)

Recommended Citation

Todd B. Sauke, J. F. Becker, and M. Loewenstein. "Stable isotope analysis using tunable diode laser spectroscopy" *Applied Optics* (1992): 1921-1927.

This Article is brought to you for free and open access by the Physics and Astronomy at SJSU ScholarWorks. It has been accepted for inclusion in Faculty Publications by an authorized administrator of SJSU ScholarWorks. For more information, please contact scholarworks@sjsu.edu.

Stable isotope analysis using tunable diode laser spectroscopy

Joseph F. Becker, Todd B. Sauke, and Max Loewenstein

Measurements of ratios of stable isotopes are used in such diverse fields as petroleum prospecting, medical diagnostics, and planetary exploration. The narrow emission linewidth available from tunable diode lasers permits high-resolution infrared absorption measurements of closely spaced isotopic rovibrational lines. Our dual beam spectrometer uses the sweep integration technique in a spectral region where adjacent spectral lines are of approximately equal absorbance at the expected isotopic abundances. The experimental results reported here indicate that isotopic ratios of carbon in carbon dioxide can be measured to an accuracy of better than 0.4%. This laser spectroscopic technique offers an alternative to the mass spectrometric technique for *in situ* isotopic analysis in field studies, as well as flight and space applications.

Key words: Diode laser, isotopic ratio, $^{13}\text{C}/^{12}\text{C}$, carbon dioxide, laser spectroscopy.

I. Introduction

Variations in ratios of stable carbon isotopes have provided a wealth of information concerning the origin and the history of carbon-containing material.^{1,2} Reaction rates of ^{12}C differ from those of ^{13}C owing to the kinetic isotope effect.³ For example, when carbon dioxide is fixed during green plant photosynthesis, an approximately 2%–3% decrease of $^{13}\text{C}/^{12}\text{C}$ occurs in most plants.⁴ Reaction conditions, such as temperature and pressure, can influence the $^{13}\text{C}/^{12}\text{C}$ ratio in the products. Also, geological processing can mix deposits, affecting isotopic ratios. Typical variations among different inorganic deposits are up to several tenths of one percent, and, among organic deposits, the variations are even greater.¹ Thus, it is possible to use the isotopic ratio measurements of carbon in such diverse samples as rocks, soil, and expired breath from animals to gain insight into the origin of the carbon or the conditions under which the samples were formed. For example, $^{13}\text{C}/^{12}\text{C}$ measure-

ments help to trace the sources of petroleum and natural gases.⁵

By using a tunable diode laser (TDL) spectrometer to record absorption spectra of $^{12}\text{CO}_2$ and $^{13}\text{CO}_2$ infrared lines, we can measure the isotopic ratio of the carbon in a sample. The usual method of measuring $^{13}\text{C}/^{12}\text{C}$ ratios is by the well-accepted mass spectrometric technique.^{6,7} This method is extremely accurate but requires substantial sample preparation and purification to obtain reliable results.⁸ At the high spectral resolution provided by semiconductor diode lasers, problems of impurity gas interference with the measurement are essentially eliminated. The narrow spectral lines of impurity gases, such as H_2O , CH_4 , O_3 , and N_2O , for example, tend to lie far from the narrow rovibrational lines of the CO_2 gas being studied. This represents a major advantage over the mass spectrometric technique for measuring isotopic ratios. For example, organic material could be reacted under either oxidizing or reducing conditions, and the resulting gases analyzed directly without the additional purification steps required for mass spectrometric analysis. This is an important advantage for *in situ* analysis and remote applications such as planetary exploration missions. Tunable diode lasers are well suited in general for space and flight applications and are currently in use in several flight instruments, for example, the airborne tunable laser absorption spectrometer (ATLAS).⁹

In this paper we describe an optical technique to measure $^{13}\text{C}/^{12}\text{C}$ ratios in CO_2 by TDL laser spectroscopy. The technique, as well as the optical system,

J. F. Becker is with the Department of Physics, San Jose State University, 1 Washington Square, San Jose, California 95192-0106. T. B. Sauke is with the Solar System Exploration Branch, Ames Research Center, National Aeronautics and Space Administration, Moffett Field, California 94035. M. Loewenstein is with the Atmospheric Chemistry and Dynamics Branch, Ames Research Center, National Aeronautics and Space Administration, Moffett Field, California 94035.

Received 8 January 1991.

0003-6935/92/121921-07\$05.00/0.

© 1992 Optical Society of America.

data acquisition, and data analysis are described and discussed. Preliminary experimental results are also presented.

II. Experimental Methods

Several approaches that use (TDL's) for carbon isotopic analysis have been reported.¹⁰⁻¹³ The present research uses a technique proposed in 1981 by Wall *et al.*,¹² which involves the use of absorption lines of ¹²CO₂ and ¹³CO₂ in the 4.3- μ m vibrational bands. In the spectral region where the ν_3 bands of the two isotopes overlap, certain closely spaced ¹²CO₂ and ¹³CO₂ rovibrational spectral lines have approximately equal absorbance at the anticipated $\sim 1:90$ isotopic ratio, as shown in Fig. 1. Several isotopic line pairs are suitable, such as the *R*(10) line of ¹³CO₂ at 2291.681 cm⁻¹ and the *P*(60) line of ¹²CO₂ at 2291.542 cm⁻¹, both of the ν_3 fundamental band of CO₂. These two lines are separated by only 0.139 cm⁻¹ but can be well resolved by using a TDL. Comparing the absorptions of such a line pair yields a measure of the isotopic ratio in the sample gas. It is important for the isotopic lines to have approximately equal absorbances so that measurement errors can be minimized.

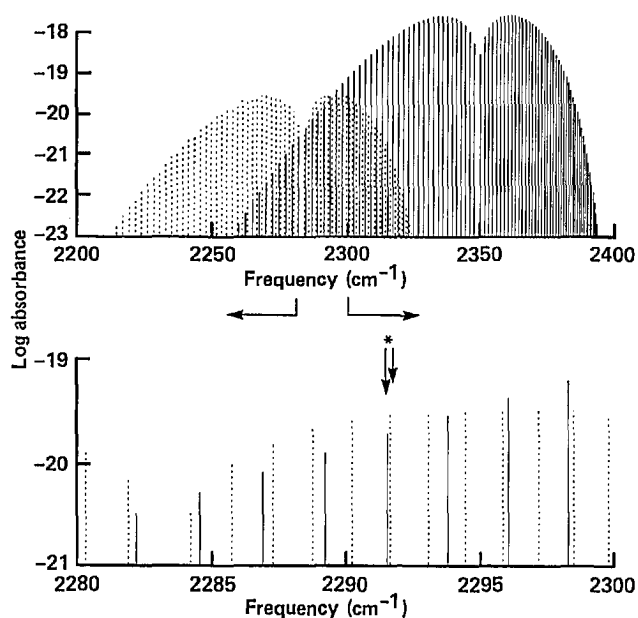


Fig. 1. Upper graph, integrated absorbances [cm⁻¹/(molecule cm⁻²)] of individual rovibrational lines from the ν_3 bands of ¹³CO₂ (dashed lines) and ¹²CO₂ (solid lines). The relative absorbance of the lines is indicated for an isotopic ratio (¹³C/¹²C) of $\sim 1:90$ as is the case for Earth samples. The bands overlap in such a way as to have approximately equal absorbances for the two isotopes in the region from ~ 2280 to ~ 2300 cm⁻¹. Lower graph, expanded plot of the overlap region of the ν_3 bands of ¹³CO₂ (dashed lines) and ¹²CO₂ (solid lines). A particularly suitable pair of ¹³C/¹²C lines is indicated by an asterisk. The *R*(10) line of ¹³CO₂ and the *P*(60) line of ¹²CO₂ are only 0.139 cm⁻¹ apart and have nearly equal absorbances. These two lines may be scanned in one sweep and the relative absorbances measured can be used to determine the isotopic composition. Representative spectra of these lines are shown in Figs. 4 and 5.

The TDL spectrometer used in our laboratory is a modified Model LS-3 (Laser Photonics, Analytics Division, Bedford, Mass. 01730) and is shown schematically in Fig. 2. The diode lasers (model L5621, Laser Photonics, Analytics Division, Bedford, Mass. 01730) used in the spectrometer were of the buried heterostructure type fabricated by the molecular beam epitaxy technique and were composition tuned to operate in the region 2290–2305 cm⁻¹. These diodes have only recently become commercially available and are an important component in achieving highly accurate measurements. They operate at temperatures above 77 K, eliminating the need for a closed cycle helium refrigerator with its associated mechanical vibrations, and they have improved single-mode emission characteristics compared with previously available diodes. The operating frequency of the laser output is tuned by varying the diode temperature and the injection current. The laser beam is passed through a 0.5-m Czerny–Turner grating monochromator to ensure isolation of a single laser mode. The laser beam is split with a pellicle beam splitter, and the two beams are directed through identical sample and reference gas cells, each having a 16-cm path length and barium fluoride windows. The liquid-nitrogen cooled indium antimonide detectors (Infrared Associates, Cranbury, N.J. 08512) are dc coupled into a transimpedance preamplifier. The amplified signals from the detectors are fed into a 12-bit, 100-kHz, analog-to-digital converter board (DAS-16F, Metrabyte Corp., Taunton, Mass. 02780) installed in an AT&T personal computer Model 6300, which is IBM PC compatible.

The laser temperature is adjusted to select an appropriate lasing mode, and the injection current is ramped so that the laser output scans across the spectral region that includes the absorption lines of interest. We achieved continuous frequency tuning in a single mode over a frequency interval greater than 5 cm⁻¹, as shown in Fig. 3. This interval includes a line pair that is appropriate for isotopic ratio determination. Verification of spectroscopic line identity was made by comparing measured spectral parameters with corresponding parameters from the HITRAN database.¹⁴

At the beginning of the current ramp, a blanking current pulse briefly turns off the laser and provides a zero signal level. The blanking pulse and the current ramp are repeated at a fixed frequency, typically between 20 and 50 Hz. The detected signal from each sweep is digitized and repeated sweeps are co-added to increase signal-to-noise ratio. This technique is known as sweep integration.¹⁵ Rapid data acquisition, at 100 k samples/s, is controlled by the built-in timing and the direct memory access circuitry on the data acquisition board, proceeding as a hardware-controlled background process. Concurrent with the data acquisition, fast assembly language subroutines perform sweep integration by co-adding the data points from each spectrum to previously acquired spectra.

The sample and the reference cell scans to be

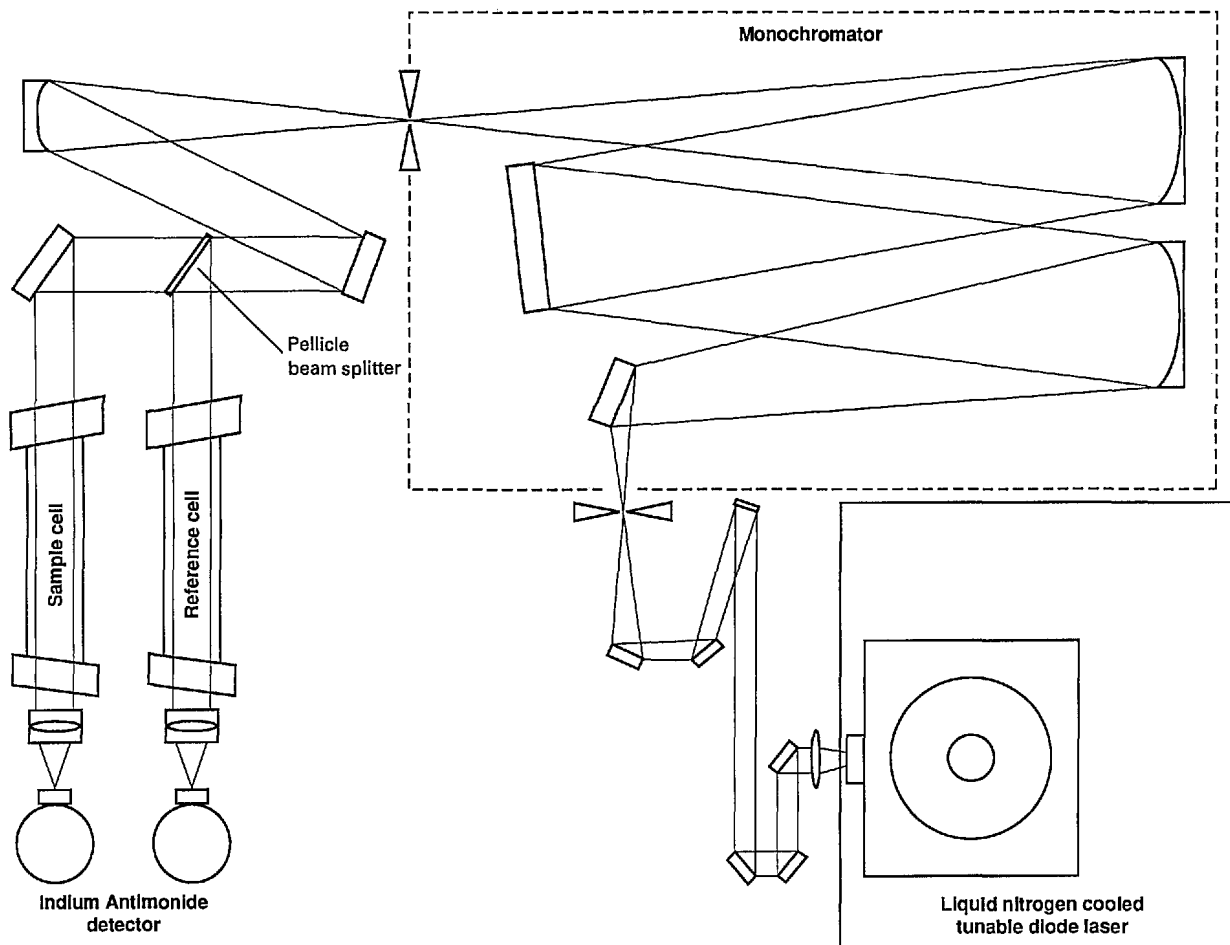


Fig. 2. Schematic of a stable isotope laser spectrometer (SILS), with a liquid-nitrogen cooled lead-salt diode laser, a grating monochromator, a pellicle beam splitter, and liquid-nitrogen-cooled indium antimonide detectors.

co-added are acquired alternately rather than strictly simultaneously. Because many individual scans (typically 512) are co-added over the data collection period, the sample and the reference data may be considered

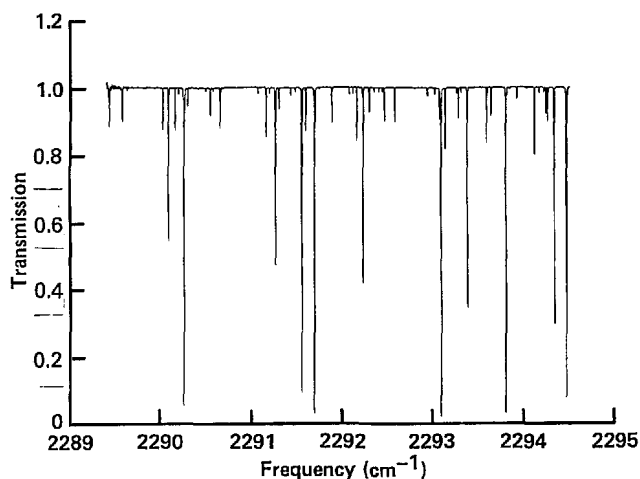


Fig. 3. Spectrum of CO₂ obtained with our spectrometer operating in a single lasing mode at 79 K. The sample CO₂ gas was at room temperature and at a pressure of 1.25 Torr. This sweep-integrated spectrum was obtained by co-adding 512 individual sweeps.

to be collected essentially simultaneously (within 100 ms).

To calibrate the wave-number scale for the spectral scan, we inserted a 25.4-mm germanium étalon (free spectral range = 0.04864 cm^{-1} in the spectral region near 2290 cm^{-1} at room temperature) into a collimated portion of the beam, and the resulting interference pattern was recorded. The free spectral range of the étalon divided by the number of data channels between successive interference maxima yields the number of wave numbers per channel as a calibration factor. A small, but significant, nonlinearity in the calibration factor from the beginning to the end of the spectrum is typically observed owing to nonlinear diode tuning rates and to the recovery of the diode from the blanking pulse. This nonlinearity can be accounted for by fitting the locations of all étalon maxima to a polynomial that can then be used to convert the data channel numbers to their corrected wave-number value.

An evacuated cell spectrum is also recorded to determine the 100% transmission as a function of wave number. In addition, laser mode purity is assessed by acquiring a high-absorbance spectrum at elevated CO₂ pressure and comparing transmission at

the saturated absorbance peak with the zero signal level. The above spectral calibration scans are used in the analysis of the experimental data. Typical spectra are shown in Fig. 4. Mode purity can be assessed by noting how closely the high-pressure (saturated) lines approach zero transmission. The transmission at the centers of saturated absorption lines is typically $\sim 0.2\%$. It can be shown that the extended wings of even a single narrow Lorentz laser emission line can contribute to measurable deviations from zero transmission at the saturated centers of absorption lines.¹⁶ Most of the 0.2% transmission at saturated line centers can be attributed to this source, implying that mode impurities contribute much less than 0.2% to our measured signal. The absolute wave-number axis, as determined by the étalon spectrum and known spectral line frequencies, is estimated to be accurate to better than 0.0002 cm^{-1} . Another data set and its calibration scans are also obtained from the second (reference) beam. If the isotopic composition of the gas in the second cell is known, these data can be used as a reference to determine the isotopic composition of the sample gas.

The data are subsequently transferred to a DEC

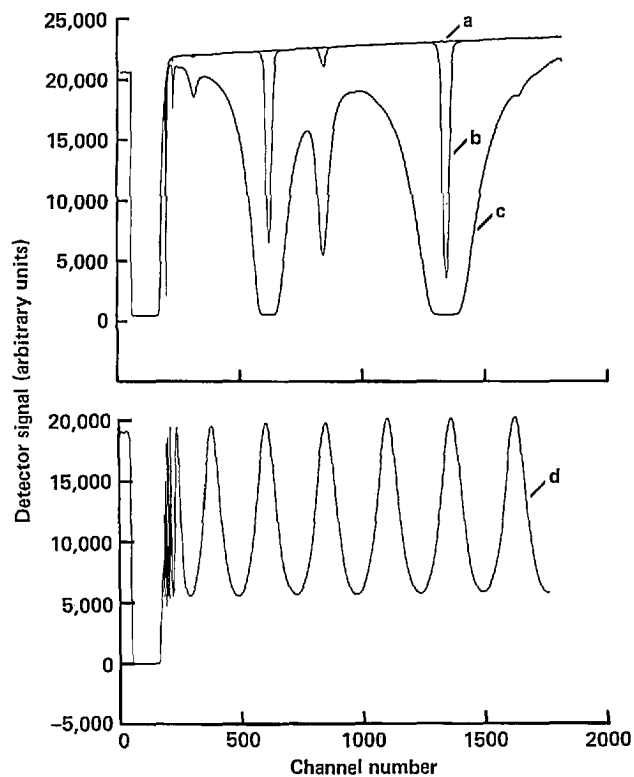


Fig. 4. Raw spectra covering the region of the $^{13}\text{CO}_2$ $R(10)$ and $^{12}\text{CO}_2$ $P(60)$ spectral lines of the ν_3 rovibrational band. Each spectrum consists of 512 co-added sweeps. a, Evacuated cell indicating 100% transmission; b, spectrum of CO_2 lines at 0.77 torr; c, spectrum of CO_2 lines at high pressure (high absorbance) (the saturated absorbance peaks indicate zero transmission); d, spectrum of the germanium étalon inserted into the beam of the evacuated cell. The accurate wave-number spacing of the interference fringes (0.04864 cm^{-1} per fringe) permits a reconstruction of the corrected wave-number axis.

MicroVAX computer and analyzed by using programs written in Interactive Data Language (Research Systems, Inc., Boulder, Colo. 80207). The data are fitted in transmission space to a mathematical model that consists of Voigt profiles that have been transformed from absorption space to transmission space. The parameters varied in the nonlinear least-squares fit are the Doppler and the Lorentz linewidths, the strength, and the peak location of each absorption line. The analytic function for the Voigt profile is the real part of the complex error function for which there exists an accurate and well-accepted rational fraction approximation.¹⁷

Specifically, in the present case our data scans were selected to include the $^{13}\text{CO}_2$ $R(10)$ and $^{12}\text{CO}_2$ $P(60)$ ν_3 fundamental rovibrational absorption lines that are suitable for isotopic ratio measurements when our system is used. A typical spectrum of this pair is shown in Fig. 5. The transmission data shown (which are equal to the ratio of the raw data scan and the evacuated, 100% transmission scan shown in Fig. 4) were fit to three Voigt profiles on a linear baseline. A correction of the nonuniformity in the frequency interval between data points was performed as indicated above. Also shown in Fig. 5 is a plot of the fit, which lies too close to the data to be distinguished on this scale, and the residual (data minus fit) times 10.

The areas (in absorbance units) of the $^{13}\text{CO}_2$ and $^{12}\text{CO}_2$ lines can be determined from the Voigt fitting parameters. The ratio of the line absorbances of gas

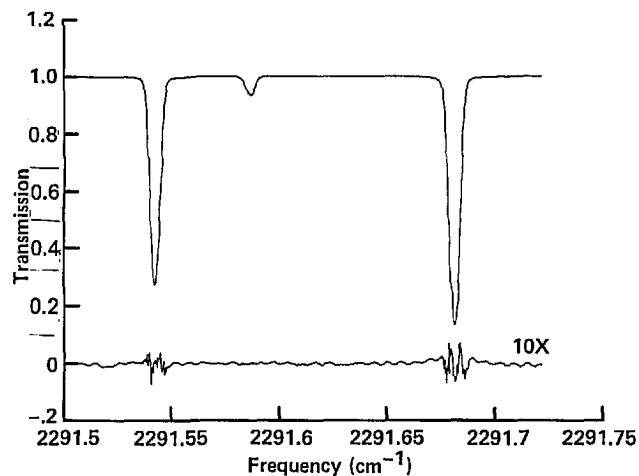


Fig. 5. Transmission spectrum of the CO_2 lines shown in Fig. 4. This spectrum is the ratio of the raw data spectrum and the raw evacuated cell spectrum yielding the transmission. The zero transmission level has been shifted by taking into account the saturated spectrum of Fig. 4 (spectrum c), which indicated $\sim 0.2\%$ background signal at the saturated absorption line center, possibly from mode impurities or laser line Lorentz tails. The wave-number axis has been assigned by taking into account the étalon sweep shown in Fig. 4, spectrum d. The data have a signal-to-noise ratio of several thousand. Also shown is a plot of the fit to the data, which lies too close to the data to be distinguished in this figure. The residual (data minus fit) times 10 is plotted below. The small systematic deviations between data and fit presumably are due to instrumental imperfections, for example, the small but detectable width of the instrument response function.

in the sample cell divided by the ratio of the line absorbances of gas in the reference cell under the same conditions is equal to the ratio of their $^{13}\text{CO}_2/^{12}\text{CO}_2$ ratios, leading to the percent difference of their isotopic composition. If the gas in the reference cell is of known isotopic composition, a measurement of absolute isotopic ratio in the unknown sample is possible. It is important that the sample and the reference scans be measured essentially simultaneously; many systematic measurement errors tend to cancel in the ratio, resulting in improved accuracy.

The Doppler widths retrieved in typical scans are approximately 2% greater than the theoretical values, and the retrieved Lorentz width (which should be smaller than 10^{-4} cm^{-1} at our typical sample pressures of less than 1 Torr) are $\sim 1.5\text{--}2.5 \times 10^{-4} \text{ cm}^{-1}$. These excess broadenings are caused by various instrumental effects that together define the instrument response function (IRF) of the spectrometer system. We attribute the excess Lorentz width to the linewidth of the diode laser itself. Conventional theories¹⁸⁻²⁰ of laser linewidths indicate that our diode laser linewidth should be of the order of 10^{-5} cm^{-1} . However, measured diode laser linewidths have been found to be substantially broader than theoretical values.²¹⁻²⁵ Several authors²⁶⁻³⁰ have proposed theories that successfully account for the enhanced Lorentzian broadening of the laser line. The extra broadening of our measured Doppler widths can be attributed to an approximately Gaussian contribution to the overall IRF with a width of approximately 0.0004 cm^{-1} . Preliminary evidence indicates that the source of this extra broadening is due largely to random current noise in the injection current ramp generator. Taking the effects of these contributions together, the overall IRF appears to have a total width of approximately 0.0005 cm^{-1} , indicating the maximum instrumental resolution that can currently be obtained with this spectrometer.

The broadening effect of the IRF on the measured spectra introduces systematic line-shape errors. Because the isotopic ratio measurements reported here are based on the areas of the fitted lines rather than on the line center absorbances, systematic errors caused by the IRF are substantially reduced. However, for highly accurate quantitative results, even small systematic errors should be taken into account. We anticipate further improvements in the accuracy of future isotopic ratio determinations when the systematic errors caused by the IRF are appropriately incorporated into the data-fitting model.

III. Experimental Description and Results

To assess the accuracy of the isotopic ratio measurements, two sets of data were acquired. In the first dataset, we used identical gas samples as unknown and reference in the two sample cells. The ratio of the line absorbance ratios should theoretically be unity. Fluctuations of this calculated quantity and any systematic deviations from unity indicate the level of uncertainty in the measurement. In the second data-

set, different gas samples were used in the two sample cells: the unknown came from a source known to be enriched in $^{13}\text{CO}_2$ and the reference was unenriched. The measured isotopic enrichment of the unknown relative to the reference gas was then compared with the corresponding measurement performed by mass spectrometry.

In the first data set, 11 series of 20 spectra were recorded. The gas cells were evacuated and then refilled with gas from an identical source between runs; this simulated the loading of a new unknown sample (and new reference gas). The reproducibility of the spectral parameters of the lines was determined within each run. The standard deviation of the individual strengths of the two lines of interest was better than 1%, and that of the Doppler widths was better than 0.5%. The measured line separation of the two lines was reproducible to within $\sim 0.0002 \text{ cm}^{-1}$. The isotopic ratio results from the 11 measurement runs are shown in Table I. The standard deviation of the ratio of $^{13}\text{CO}_2/^{12}\text{CO}_2$ ratios within each run was typically better than 0.4%. The difference between the overall average and the theoretically expected value of unity is 0.4%. This is an indication of the magnitude of a systematic bias in the measurement. The standard deviation of the 11 mean ratios is 0.20%.

One might have expected that the standard deviation for values that are the average of 20 measurements would be smaller than the standard deviation of individual measurements by a factor of the square root of 20 (~ 4.5). The fact that it is only a factor of 2 improved indicates that the measurement errors are not purely statistical and are dominated by systematic errors and instrumental drifts. Part of the systematic inaccuracy can be attributed to the effects of unequal temperatures in the two gas cells during data acquisition. Because the line strength is a function of temperature and J quantum number,³¹ the ratio of two lines with significantly different J values will have a strong temperature dependence. Thus, a change of 1 K at room temperature results in a

Table I. Mean Values and Standard Deviations of 20 Measured Ratios, $(^{13}\text{CO}_2/^{12}\text{CO}_2)_{\text{unknown}} / (^{13}\text{CO}_2/^{12}\text{CO}_2)_{\text{ref}}$ in Eleven Pairs of Identical Gas Samples^a

Run	Mean of 20	Standard Deviation of 20
1	1.0018	0.0031
2	1.0031	0.0035
3	0.9999	0.0039
4	1.0038	0.0039
5	1.0050	0.0050
6	1.0029	0.0040
7	1.0044	0.0026
8	1.0030	0.0027
9	1.0080	0.0030
10	1.0027	0.0021
11	1.0047	0.0024
Overall mean	1.0036	0.0033

^a $P = 0.6 \text{ Torr}$, $T \sim 293 \text{ K}$.

Table II. Mean Values and Standard Deviations of 20 Measured Ratios, $(^{13}\text{CO}_2/^{12}\text{CO}_2)_{\text{unknown}}/(^{13}\text{CO}_2/^{12}\text{CO}_2)_{\text{ref}}$, in Four Pairs of Sample-Reference Gases^a

Run	Mean of 20	Standard Deviation of 20
1	1.0506	0.0029
2	1.0565	0.0035
3	1.0521	0.0025
4	1.0480	0.0025
Overall mean	1.0518	0.0029

^aFor comparison, the actual isotopic enrichment, as determined by mass spectrometry, is 1.0525 ($P = 0.6$ Torr, $T \sim 293$ K).

change of approximately 2% in the absorbance ratio of lines such as the $R(J = 10)/P(J = 60)$ pair.

Table II shows the results of the second data set in which the unknown sample was enriched in $^{13}\text{CO}_2$. The standard deviation of the ratio of $^{13}\text{CO}_2/^{12}\text{CO}_2$ ratios within each run was better than 0.4%. The average value determined for the percent of $^{13}\text{CO}_2$ isotopic enrichment was 5.18 (average deviation 0.3). The actual percent of isotopic enrichment, as determined by mass spectrometry,³² was 5.25 ± 0.01 .

IV. Conclusion

Ratios of $^{13}\text{C}/^{12}\text{C}$ in carbon dioxide have been measured with our TDL spectrometer to a present accuracy of better than 0.4%. These results were made possible by using state-of-the-art high-temperature TDL's, an étalon and wave-number calibration technique, high-speed assembly language controlled data acquisition, and the ratioing of absorbances from simultaneously acquired sample and reference data scans. Increased accuracy will result from improvements in temperature stabilization of the gas cells and by incorporating the IRF into the data-fitting model to account for known instrumental distortions. The data for an individual ratio determination are obtained over a time of less than 1 min, while the sequence of 20 pairs of spectra was obtained over a time of approximately 30 min. The length of time required to acquire the data can be drastically reduced by more efficient data file handling and by use of a faster computer. Because the accuracy of the present measurement is limited by systematic rather than statistical errors, the number of co-added scans per spectrum can be reduced to speed up the data acquisition without seriously compromising the accuracy. In fact, faster data acquisition may improve accuracy by limiting the time over which system drifts can occur. Overall optimization in choice of sample pressure, scanning repetition rate, number of scans to signal average, and other experimental details should yield further improvements in accuracy and speed. It is expected that these and other improvements in technique that we are now implementing will permit determinations of isotopic ratios to better than 0.1% for measurement times substantially shorter than 1 min, perhaps several seconds. This

laser technique permits isotopic ratios to be measured without the extensive sample purification required for mass spectrometric analysis; many of the commonly expected impurity gases can be present in the sample without adversely affecting the measurement. By optimizing sample cell configuration, the amount of carbon required to make an isotopic ratio determination can be less than a microgram. The rugged, lightweight, and reliable TDL is ideally suited for use in instruments both in the laboratory and in the field. TDL spectroscopy should prove to be a useful technique for *in situ* measurements of isotopic ratios in such diverse fields as medical diagnostics by using expired CO_2 in human breath, petroleum exploration, and planetary exploration missions.

The authors thank Thomas Gutierrez for his help with data acquisition and analysis. The mass spectrometric analysis was generously provided by David DesMarais. This research was supported in part by the National Aeronautics and Space Administration's (NASA's) Exobiology Flight Program, the Solar System Exploration Branch at NASA Ames Research Center, NASA grant NCA2-407 and NSF-REU grant PHY90-00697. This research was performed while Todd Sauke was supported by a National Research Council NASA postdoctoral fellowship.

References

1. M. Schidlowski, J. M. Hayes, and I. R. Kaplan, "Isotopic inferences in ancient biochemistries: carbon, sulfur, hydrogen, and nitrogen," in *Earth's Earliest Biosphere, Its Origins and Evolution*, J. W. Schopf, ed. (Princeton U. Press, Princeton, N.J., 1983).
2. D. J. DesMarais and J. G. Moore, "Carbon and its isotopes in mid-oceanic basaltic glasses," *Earth Planet. Sci. Lett.* **69**, 43-57 (1984).
3. L. Melander and W. H. Saunders, *Reaction Rates of Isotopic Molecules* (Wiley, New York, 1980).
4. M. H. O'Leary, "Carbon isotope fractionation in plants," *Phytochemistry* **20**, 553-567 (1981).
5. B. P. Tissot and D. H. Welte, *Petroleum Formation and Occurrence* (Springer-Verlag, Berlin, 1984).
6. A. O. Nier, "A mass spectrometer for isotope and gas analysis," *Rev. Sci. Instrum.* **18**, 398-411 (1947).
7. D. E. Matthews and J. M. Hayes, "Isotope-ratio-monitoring gas chromatography-mass spectrometry," *Anal. Chem.* **50**, 1465-1473 (1978).
8. K. W. Wedeking, J. M. Hayes, and U. Matzigkeit, "Procedures of organic geochemical analysis," in *Earth's Earliest Biosphere, Its Origins and Evolution*, J. W. Schopf, ed. (Princeton U. Press, Princeton, N.J., 1983).
9. M. Lowenstein, J. R. Podolske, K. R. Chan, and S. E. Strahan, "Nitrous oxide as a dynamical tracer in the 1987 airborne antarctic ozone experiment," *J. Geophys. Res.* **94**, 11,589-11,598 (1989).
10. G. J. Kemeny, R. S. Eng, and A. W. Mantz, "Utilization of tunable infrared diode lasers for the determination of labelled molecules in gas mixtures," *Acta Phys. Acad. Sci. Hung.* **48**, 93-102 (1980).
11. D. Labrie and J. Reid, "Radiocarbon dating by infrared laser spectroscopy—a feasibility study," *Appl. Phys.* **24**, 381-386 (1981).
12. D. L. Wall, R. S. Eng, and A. W. Mantz, "Development of a

- tunable diode laser isotope ratio measurement system," presented at the Thirty-second Pittsburgh Conference on Analytical Chemistry and Applied Spectroscopy, Pittsburgh, Pa., March, 1981.
13. P. S. Lee and R. F. Majkowski, "High resolution infrared diode laser spectroscopy for isotope analysis-measurement of isotopic carbon monoxide," *Appl. Phys. Lett.* **48**, 619-621 (1986).
 14. L. S. Rothman, R. R. Gamache, A. Goldman, L. R. Brown, R. A. Toth, H. M. Pickett, R. L. Poynter, J-M. Flaud, C. Camy-Peyret, A. Barbe, N. Husson, C. P. Rinsland, and M. A. H. Smith, "The HITRAN database: 1986 edition," *Appl. Opt.* **26**, 4058-4097 (1987).
 15. D. E. Jennings, "Absolute line strengths in ν_4 $^{12}\text{CH}_4$: a dual-beam diode laser spectrometer with sweep integration," *Appl. Opt.* **19**, 2695-2700 (1980).
 16. J. R. Podolske, Atmospheric Chemistry and Dynamics Branch, Ames Research Center, National Aeronautics and Space Administration, Moffett Field, Calif. 94035 (personal communication).
 17. A. K. Hui, B. H. Armstrong, and A. A. Wray, "Rapid computation of the Voigt and complex error functions," *J. Quant. Spectrosc. Radiat. Transfer* **19**, 509-516 (1977).
 18. A. L. Schawlow and C. H. Townes, "Infrared and optical masers," *Phys. Rev.* **112**, 1940-1949 (1958).
 19. M. Lax, "Classical noise. V. Noise in self-sustained oscillators," *Phys. Rev.* **160**, 290-307 (1967).
 20. R. D. Hempstead and M. Lax, "Classical noise. VI. Noise in self-sustained oscillators near threshold," *Phys. Rev.* **161**, 350-366 (1967).
 21. J. J. Hillman, D. E. Jennings, and J. L. Faris, "Diode laser- CO_2 laser heterodyne spectrometer: measurement of $2sQ(1, 1)$ in $2\nu_2 - \nu_2$ of NH_3 ," *Appl. Opt.* **18**, 1808-1811 (1979).
 22. M. W. Flemming and A. Mooradian, "Spectral characteristics of external-cavity controlled semiconductor lasers," *IEEE J. Quantum Electron.* **QE-17**, 44-59 (1981).
 23. D. Welford and A. Mooradian, "Output power and temperature dependence of the linewidth of single-frequency CW (GaAl)As diode lasers," *Appl. Phys. Lett.* **40**, 865-867 (1982).
 24. Y. Kotaki and H. Ishikawa, "Spectral characteristics of a three-section wavelength-tunable DBR laser," *IEEE J. Quantum Electron.* **25**, 1340-1345 (1989).
 25. A. Hemmerich, D. H. McIntyre, D. Schopp, Jr., D. Meschede, and T. W. Hansch, "Optically stabilized narrow linewidth semiconductor laser for high resolution spectroscopy," *Opt. Commun.* **75**, 118-122 (1990).
 26. C. H. Henry "Theory of the linewidth of semiconductor lasers," *IEEE J. Quantum Electron.* **QE-18**, 259-264 (1982).
 27. C. H. Henry "Theory of the phase noise and power spectrum of a single mode injection laser," *IEEE J. Quantum Electron.* **QE-19**, 1391-1397 (1983).
 28. C. Freed, J. W. Bielinski, and W. Lo, "Fundamental linewidth in solitary, ultra-narrow output $\text{PbS}_{1-x}\text{Se}_x$ diode lasers," *Appl. Phys. Lett.* **43**, 629-631 (1983).
 29. G. Bjork and O. Nilsson, "A tool to calculate the linewidth of complicated semiconductor lasers," *IEEE J. Quantum Electron.* **QE-23**, 1303-1313 (1987).
 30. J. Arnaud "Contribution of shot noise to laser diode linewidth," *Opt. Commun.* **68**, 423-426 (1988).
 31. S. S. Penner, *Quantitative Molecular Spectroscopy and Gas Emissivities* (Addison-Wesley, Reading, Mass. 1959).
 32. D. J. DesMarais, Planetary Biology Branch, Ames Research Center, National Aeronautics and Space Administration, Moffett Field, Calif. 94035 (personal communication).